Ocean Science

Acoustic Doppler current profiler observations of migration patterns of zooplankton in the Cretan Sea

Emmanuel Potiris[1,2], Constantin Frangoulis[1], Alkiviadis Kalampokis[1], Manolis Ntoumas[1], Manos Pettas[1], George Petihakis[1], and Vassilis Zervakis[2]

[1]Institute of Oceanography, Hellenic Centre for Marine Research, Heraklion, Crete, 72100, Greece
[2]Department of Marine Sciences, School of the Environment, University of the Aegean, Mytilene, Lesvos, 81132, Greece

Correspondence: Emmanuel Potiris (mpotiris@hcmr.gr)

Abstract. The lack of knowledge of the mesopelagic layer inhabitants, especially those performing strong vertical migration, is an acknowledged challenge. This incomplete representation leads to the exclusion of an active carbon and nutrient pathway from the surface to the deeper layers and vice versa. The vertical migration of mesopelagic inhabitants (macroplanktonic and micronektonic) was observed by acoustical means for almost 2.5 years in the epipelagic and mesopelagic layers of the open oligotrophic Cretan Sea (south Aegean Sea, eastern Mediterranean) at the site of an operational fixed-point observatory located at 1500 m depth. The observed organisms were categorized into four groups according to their migration patterns. The variability of the migration patterns was inspected in relation to the physical and biological environmental conditions of the study area. The stratification of the water column does not act as a barrier for the vertical motion of the strongest migrants that move up to 400 m every day. Instead, changes in light intensity (lunar cycle, daylight duration, cloudiness) and the presence of prey and predators seem to explain the observed daily, monthly and seasonal variability. The continuous presence of these organisms, which are capable of vertical motion despite the profound circulation variability at the site of the observatory, implies their presence in the broader study area. The fundamental implications of the above regarding biogeochemical processing in oligotrophic seas due to the intimate link between the carbon (C) and nutrient cycles, are discussed.

1 Introduction

The biological organic carbon pump is the major oceanic process that photosynthetically converts the dissolved CO_2 in the surface layers of the ocean to particulate organic carbon. This organic carbon is then consumed by pelagic biota, and exported to depth by a combination of sinking particles, advection or vertical mixing of dissolved organic matter and transport by animals (Turner, 2015). Buesseler and Boyd (2009) noted that "the surface ocean" is "where the "strength" of the biological pump is set" whereas "the subsurface ocean" is "where the "efficiency" of the biological pump is determined".

The main factor determining the biological pump's efficiency in the mesopelagic and bathypelagic zones, is the organic carbon export carried out by sinking and vertical migration by zooplankton and fish, in combination with microbial degradation. The diel vertical migration (DVM) of zooplankton, i.e., their vertical movement in the water column within the 24 h day, creates an active flux, pumping carbon between the epipelagic and mesopelagic layers (review by Turner, 2015). The most common pattern regarding the DVM of zooplankton is a single descent to maximum depth during daytime, and a single ascent to minimum depth during nighttime (review by Cohen and Forward, 2009). DVM is a behavioral response that has been related to several exogenous (light, temperature, salinity, oxygen, hydrostatic pressure, stratification) and endogenous (sex, age, state of feeding, biological rhythm) factors (review by Forward, 1988; van Haren, 2014, and references therein). Light has emerged as the major external factor controlling DVM behavior (review by Cohen and Forward, 2009), although it is insufficient

to explain some cases where DVM occurs at depths below 1000 m, where light cannot penetrate (van Haren, 2014, and references therein).

There are also still gaps in the knowledge regarding midwater depths, which severely limit our ability to quantify the efficiency of the biological pump (Robinson et al., 2010). Concerning zooplankton DVM, one of the methodological limitations is that the populations of large individuals (macrozooplankton) that belong to important and common predatory groups capable of strong migrations, such as the chaetognaths, amphipods, euphausiids, decapods, have been underestimated. This is due to the fact that many of them escape the standard 200 µm mesh size net when towed at the recommend speed of less than $1 \, \text{m s}^{-1}$ (Moriarty and O'Brien, 2013). However, such large individuals can be detected by low frequency Acoustic Doppler current profilers (ADCPs hereafter).

Progress in ocean acoustics and marine technology during the early 1980s (Costello et al., 1989; Holliday, 1977; Holliday and Pieper, 1980; Holliday et al., 1989) allowed for the estimation of distribution patterns and biomass of zooplankton and micronekton to be inferred from ADCPs (Flagg and Smith, 1989). To measure currents, ADCPs transmit sound pulses in different directions. The sound is scattered by particulate matter in the water column, and radial velocities are computed from the Doppler shift of the backscattered signal (Gordon, 1996). The intensity of the backscattered sound can also be used in conjunction with net samples for estimating the biomass of zooplankton (Ashjian et al., 2002). Whilst the estimated ADCP backscatter is a by-product (Bozzano et al., 2014), meaning that it is more suitable for qualitative than quantitative analysis (Brierley et al., 1998), field studies complemented with ADCP-derived sound scattering have been used to describe biological patterns in the interior of the ocean, such as zooplankton aggregations (Zhou and Dorland, 2004) and vertical migration (Postel et al., 2007), in remarkable detail.

In the Mediterranean Sea, there have been several studies on vertically migrating zooplankton (see Table 5 in Andersen et al., 2001), and some have shown a substantial contribution to the total carbon export in deep waters via the active transport of migrants (Isla et al., 2015, and references therein). However, these Mediterranean DVM studies have mainly been based on net sampling for short total sampling periods (e.g., discontinuous sampling at a monthly frequency or continuous sampling for a few weeks). It is worth noting that studies of macrozooplankton are far less common than those regarding mesozooplankton, and that even for mesozooplankton there are very few interannual-scale studies in the open Mediterranean Sea (Siokou-Frangou et al., 2010). Among the Mediterranean DVM studies, the majority has been centered in the western Mediterranean (see Table 5 in Andersen et al., 2001; review by Saiz et al., 2014). These studies have pointed out different species-dependent migrating strategies, with some species migrating upwards and oth-

ers downwards at night, as well as a within species age–depth and sex–depth differential distribution. These observations were made in both the eastern and western Mediterranean (Andersen et al., 2001; Fragopoulu and Lykakis, 1990). The only DVM study in the Cretan Sea (Heraklion Bay) upper slope (300 m sea bottom) studied near-bottom macrozooplankton, and reported a reversed DVM, i.e., downward migration during nighttime (Koulouri et al., 2009).

The Cretan Sea is the most voluminous and deep (2500 m) basin of the Aegean Sea and an area of intense mesoscale variability and multiple scale circulation patterns. Two mesoscale gyres form a dipole in the Cretan Sea (Cardin et al., 2003; Kassis et al., 2015; Theocharis et al., 1999), while it is also an area of intermediate and/or deep-water formation (review by Skliris et al., 2014). Such areas of water formation are key locations for the monitoring of the Mediterranean biochemical functioning (Malanotte-Rizzoli et al., 2014). Modeling studies have shown that the open Cretan Sea's biochemistry is representative of a wide area of the eastern Mediterranean varying from 0.6 to $1.6 \times 10^6 \, \text{km}^2$ depending on the variable (i.e., primary production – PP, sea surface temperature – SST, pH, O_2, NO_3, chlorophyll a) (Henson et al., 2016).

Satellite (SeaWiFS) studies of chlorophyll a (Chl a) have clustered the Cretan Sea in a wider bioprovince of the south-central and eastern Mediterranean that covers 60 % of the total Mediterranean area, and is generally characterized by oligotrophic conditions (D'Ortenzio and Ribera d'Alcalà, 2009). The presence of a deep chlorophyll maximum (DCM hereafter), a common Mediterranean feature, which deepens going eastwards (e.g., Lavigne et al., 2015; Nowaczyk et al., 2011), also characterizes the Cretan Sea and depends on the close coupling of biological and physical processes. In fact, whilst the DCM's magnitude is mainly determined by biological mechanisms, the DCM depth and structure are essentially determined by optical–physical factors (e.g., Crise et al., 1999; Mann and Lazier, 2006; Varela et al., 1994). In the Cretan Sea the vertical extent and the intensity of the mesoscale gyres, which form a dipole, govern this coupling to a large extent (Petihakis et al., 2002).

Zooplankton studies in the Cretan Sea, were only carried out on mesozooplankton (Mazzocchi et al., 1997; Siokou-Frangou et al., 1997; Siokou et al., 2013), with the exception of one study on near-bottom macrozooplankton (Koulouri et al., 2009). Mesozooplankton abundance in the Cretan Sea's epipelagic layer was found to be at the same level as in the open Ionian and Levantine seas, and community compositions have also shown significant similarities with the above areas (Siokou-Frangou et al., 2010, and references therein). Regarding deep living zooplankton, less is known for the eastern Mediterranean (review by Saiz et al., 2014), although deep living mesozooplankton stock and composition has been investigated (Siokou-Frangou et al., 1997; Siokou et al., 2013) and its importance in consuming sinking particles reported (Koppelmann et al., 2004). For deep
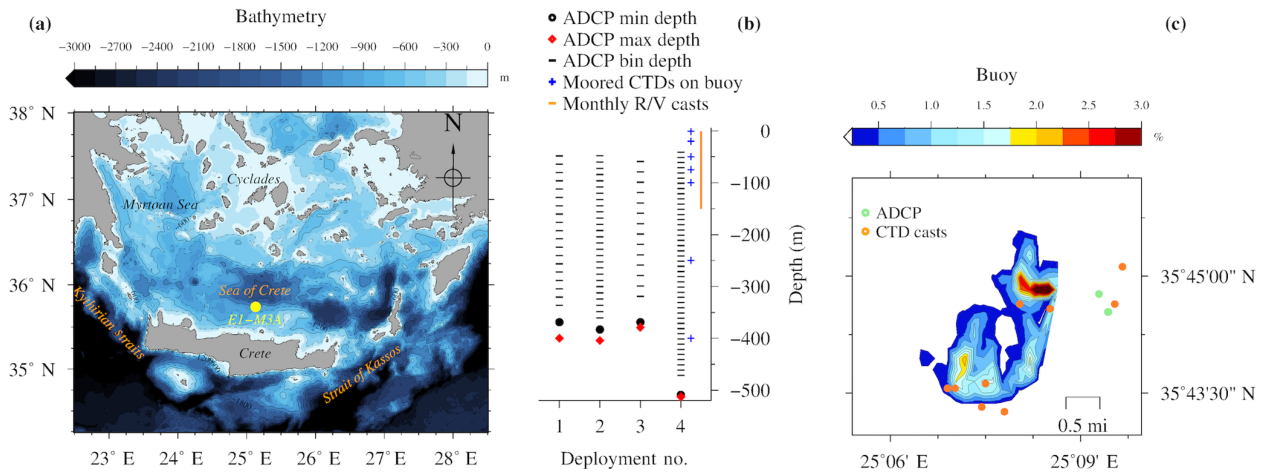
Figure 1. Topographic map of the south Aegean Sea **(a)**. Vertical **(b)** and horizontal **(c)** views of the sampling setup at E1-M3A. Details of ADCP deployments are given in Table 1. Horizontal buoy motion is shown as a percentage of the total deployment duration spent at a location.

living macrozooplankton there is even less information. The euphausiid species found in the whole Mediterranean Sea are the same, although the predominant species are different in the eastern basin and Thyrrenian Sea to those found in the western basin, west of the Thyrrenian Sea (Wiebe and D'Abramo, 1972).

ADCP studies of DVM in the Mediterranean have been limited. In the central Ligurian Sea, Bozzano et al. (2014) used an upward looking ADCP positioned at a depth of 100 m. They found that the main migration pattern is the daytime migration, in addition to the fact that deeper and stronger migration ranges are encountered during winter. In the Alboran Sea, van Haren (2014) implemented an upward looking ADCP positioned at a depth of approximately 800 m and found DVM to be related to internal waves. To our knowledge, there have been no ADCP studies of DVM in the eastern Mediterranean. However, during a study of the current velocities in the Cretan Sea in 2000, Cardin et al. (2003), using an ADCP (75 kHz), reported a noise in the measurements of vertical velocity, and migrating zooplankton was given as a possible explanation.

The present study was stimulated by this hypothesis from Cardin et al. (2003), in addition to the fact that for the 75 kHz frequency objects with a size of 5 mm (1/4 of transmit pulse wavelength) or more reflect sound and cause a strong backscatter signal (Thomson and Emery, 2001). Following this hypothesis, four consecutive deployments of the same 75 kHz ADCP were carried out at the same location as Cardin et al. (2003), covering a period of two and a half years. This provided a unique opportunity to study the migration patterns of zooplankton, continuously and at high frequency, for a long period in relation to environmental conditions. The aim of this paper is to present the observed distribution patterns of zooplankton (focusing on DVM) and discuss their relationship to physical and biological environ-

mental conditions, such as daylight, currents, stratification and food resources.

2 Materials and methods

2.1 Experimental setup

The Poseidon E1-M3A observatory (http://www.poseidon. hcmr.gr) is located at 25.12° E, 35.74° N in the center of the Cretan Sea at a depth of 1500 m (Fig. 1a). It consists of two moorings: the first has a surface buoy and a real-time multi-sensor array down to 1000 m, while the second is a subsurface mooring, hosting an upward looking RDI 75 kHz ADCP. The observation effort is complemented by monthly R/V cruises to perform conductivity, temperature and depth (CTD) casts (temperature, salinity, fluorescence) and net tows (zooplankton). The ADCP data set used in the present study consists of four successive deployments of variable duration, which extended over a period of 2 years and 6 months, from 15 November 2012 to 20 May 2015 (Table 1). The distance between the ADCP mooring line and E1-M3A buoy varied slightly but was less than 2.7 NM for all deployments (Fig. 1c). The primary purpose of the ADCP deployment was to study currents. The first deployment was considered to be a test of the setup, so the sampling scheme and the depth of the ADCP were selected empirically (Table 1). The first deployment confirmed the feasibility of monitoring biological activity and it became obvious that a greater depth should be chosen, as the parking depth of zooplankton was deeper than the initial ADCP deployment depth; the sea surface reflection also contaminated the first 50 m of the water column. However, the rearrangement of the mooring line was not possible due to the tight schedule of the next two deployments; thus,

Table 1. The deployment parameters of the upward looking 75 kHz RDI ADCP on the subsurface mooring line of E1-M3A.
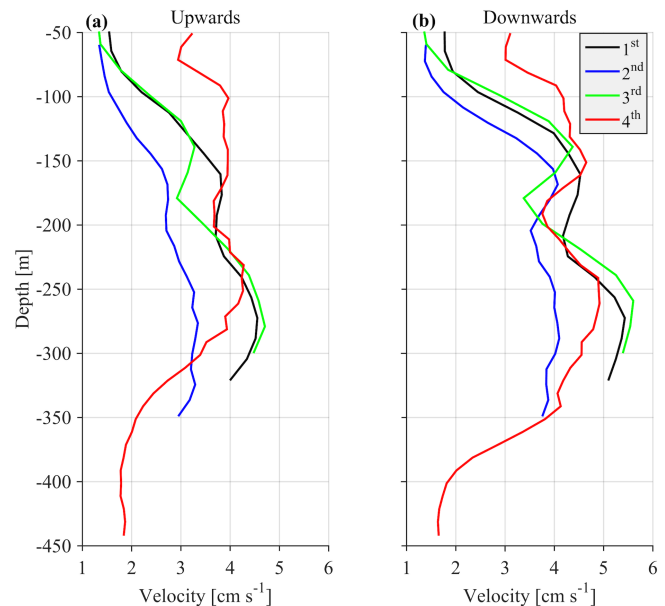
Deployment	Start	End	Bins	Bin size (m)	Sampling interval (s)	First bin (m)	Average depth (m)
First	15 Nov 2012	23 May 2013	25	16	1800	24.59	369
Second	1 Jun 2013	19 Jan 2014	33	12	3600	20.65	383
Third	19 Jan 2014	10 Oct 2014	25	20	1800	28.58	370
Fourth	10 Oct 2014	2 Jun 2015	45	10	1800	18.76	509

only the last ADCP deployment was about 120 m deeper than the previous deployments.

The ADCP sampling plan was optimized in terms of temporal and spatial resolution by setting different sampling schemes at each deployment (Table 1; Fig. 1b). The aim was to check the consistency of the vertical velocity measurements of zooplankton and the backscatter coefficient (defined in Sect. 2.2) between deployments. No significant difference in the vertical velocities or the backscatter coefficient between deployments of variable cell length and sampling rate, is an indication of reliable/accurate measurements. Thus, it is possible to identify biases caused by the sampling scheme, instead of the velocity errors due to the ADCP accuracy and the backscatter coefficient estimation methodology.

One parameter used to potentially identify the optimal cell extension and sampling interval for the most appropriate recording of zooplankton signals was the hereafter defined "burst speed". The burst speeds of each cell are defined as the highest and lowest vertical velocity measurements, respectively, during a one day time period. The velocity measurement inside a cell over the sampling interval is the result of the averaging of several pings. As the recording interval increases, the cell extension decreases and the actual zooplankton speed increases; we expect the actual zooplankton speed to be underestimated because zooplankton will not be inside the cell throughout the duration of the measurement, only during a fraction of it. The largest underestimation is expected when the actual zooplankton migration speed is at its maximum. Thus, comparison of upward and downward burst velocities between deployments at depths around 250 m (the depth at which the highest migrating speeds were recorded) were used to identify the most appropriate sampling scheme.

The challenge was to identify the lowest sampling rate that would still give an acceptable resolution for the ascending/descending zooplankton movement, while conserving power and extending the deployment period as much as possible. Two sampling and averaging intervals, of 30 min and 1 h, respectively, were tested in order to select the optimum sampling scheme. During the first deployment, a sampling interval of 30 min was used, which was subsequently followed by a 1 h interval during the second deployment. Comparison of the data from the two deployments revealed an underestimation of burst migration velocities in the second data set (Fig. 2a and b) due to the lower sampling rate

Figure 2. Time average burst velocities per ADCP deployment.

(1 h); thus, the initial value of 30 min was selected for the last two deployments.

In comparison, the range of the cells used (10–20 m) did not affect the burst speed or the average velocity measurements. Based on visual inspection, smaller cell extension during the first, third and fourth deployments (30 min sampling interval) did not result in smaller burst and average speeds. However, using a small bin size (10 m) during the last deployment resulted in noisy velocity measurements. The depth-integrated S_v (backscatter coefficient, defined in Sect. 2.2) between the depths observed for all deployments were also consistent. The seasonal variability of the physical properties of the water column affected the estimation of S_v at depths shallower than 100 m, mostly during late August. Placing the ADCP in an upward looking position at a shallower depth than the nominal range resulted in erroneous data for the first 50 m of the water column due to sound reflection from the sea surface.

2.2 Data processing/analysis and visualization of backscatter data

The backscatter coefficient $S_v \left[\mathrm{dB}\, re\, \left(4\pi\, \mathrm{m}^{-1} \right) \right]$ is given as follows:

$$S_v = C + 10\log_{10}\left((T_x + 273.16)\, R^2 \right) - L_{\mathrm{DBM}} - P_{\mathrm{DBW}}$$
$$+ 2aR + K_c\, (E - E_r), \qquad (1)$$

where C (dB) $= -159.1$ is an instrument constant, T_x (°C) is the transducer temperature, R (m) is the slant range, L_{DBM} is the $10\log_{10}$ of the transmit pulse length (m), P_{DBW} is the $10\log_{10}$ of the transmit power (W), a (dB m^{-1}) is the sound absorption coefficient, K_c is a constant of proportionality for converting the incoming raw echo data to dB, E (counts) is the raw echo data and $E_r = \min(E)$ (counts) is the reference raw echo per transducer when there is no signal. S_v was calculated according to Deines (1999), K_c according to Heywood (1996), the speed of sound for the calculation of R according to Gordon (1996) and a according to Ainslie and McColm (1998).

Instantaneous vertical velocity profiles were depth averaged and split into daily data sets to identify the hours of the day during which the zooplankton move upward or downward, as well as the seasonal and interannual variability in the ascent/descent hours. Another step was to select the maximum and minimum vertical velocities of each daily piece of data during the periods of upward and downward movement. Depending on the sampling rate, two to four samples were averaged. Finally, histograms of vertical velocity versus depth one hour before and one hour after sunrise/sunset were used to identify possible ascending/descending differences of migration patterns and evaluate the consistency between the different ADCP sampling schemes.

Climate Data Operators (CDO, 2018), Ocean Data View (Schlitzer, 2016) and Generic Mapping Tools (Wessel et al., 2013) were used for the data processing and visualization. Wind stress and sensible/latent fluxes were computed from the quality-controlled buoy data with the "air–sea" toolbox to identify the time when conditions favor the overturning of the water column (http://woodshole.er.usgs.gov/operations/sea-mat/air_sea-html/index.html, last access: 25 July 2018).

2.3 Description and processing of auxiliary data

To estimate volume backscattering, assess environmental conditions during deployments and assist with the interpretation of ADCP measurements, several complementary data sets have been used (Table 2).

The E1-M3A buoy measures meteorological variables (wind speed, gust and air temperature were used here) as well as temperature, conductivity and fluorescence at multiple depths (20, 50, 75 and 100 m). Temperature and conductivity measurements are also available at the sea surface and at a depth of 250 m. The chlorophyll concentrations are measured with the WETLabs ECO FLNTU fluorescence sensors which are mounted on the moored 16plus CTDs. A downward looking Nortek 400 kHz ADCP is mounted to the buoy hull, measuring horizontal currents at 5 m bins from the surface down to a depth of 50 m. Due to the lack of compatibility between the 400 kHz ADCP and the buoy software, backscatter measurements are not available from this instrument. The above meteorological and marine surface parameters were downloaded from the Poseidon online database (http://www.poseidon.hcmr.gr, last access: 25 July 2018), where they are stored in real time. In addition, due to occasional problems with the real-time underwater transmission, subsurface sensor data were downloaded from the memory logs of the instruments during the regular biannual maintenance. Meteorological and sea surface measurements from the buoy's sensors span a period of 24 months (from 22 May 2013 to 25 May 2015) and subsurface measurements a period of 20 months (from 22 May 2013 to 10 January 2015). Buoy data have undergone automated quality control, such as the rejection of stalled values and the application of min–max and spike filters. Visual inspection was the last quality control step; the remaining suspect measurements were removed manually. The heat flux through the air-sea interface computations were based on the air-sea interaction Matlab routines provided by Rich Pawlowitz (via the SEAMAT collection, https://sea-mat.github.io/sea-mat/, last access: 25 July 2018), applied on the E1-M3A meteorological and sea surface data.

2.4 Limitations

Several limitations of the ADCP and auxiliary data should be carefully considered. S_v is a proxy for zooplankton biomass and when integrated along the acoustical beams it can provide a gross measure of the instantaneous biomass of the water column (changes in the acoustical character of zooplankton cannot be identified). Whilst the integrated S_v is consistent among the deployments (discrepancies between deployments were only observed for the first few bins), an analysis of this description is not meaningful with the experimental configuration of this study. This is due to the fact that the zooplankton are not permanently within the range of the ADCP and because of the seasonal succession of dominant species constituting the zooplankton stocks in the Cretan Sea (Gotsis-Skretas et al., 1999). The upper 50 m of the water column are not measured, which means that the depth integrated S_v exhibits significant variability due to the monthly change in the depth to which the zooplankton ascend during nighttime because of moonlight. Furthermore, the whole deep scattering layer is only found inside the ADCP range for a small period of the fourth deployment, adding another source of variability that is not attributed to biomass changes of zooplankton. Another source of error, which largely depends on the availability of auxiliary data, is the imperfect calculation of the effects of the gradients of the upper water column in the estimation of S_v due to the changes in temperature and salinity. The above problems are generally en-

Table 2. The type, source, time coverage and resolution of the auxiliary data. In situ data have gaps of variable lengths. Monitoring by R/V refers to the monthly monitoring program of regular R/V visits to the E1-M3A observatory site. NASA refers to the Goddard Space Flight Center.

Parameter	Type	Source	Time coverage	Time resolution
Air temp & wind	In situ	E1-M3A buoy	2013/05–2014/10	3 h
Surface currents (0–50 m)	In situ	E1-M3A buoy (ADCP 400 kHz)	2013/05–2015/05	3 h
Subsurface currents (0–400 m)	In situ	ADCP (75 kHz)	2012/11–2015/05	0.5–1 h
Water temperature & salinity	In situ In situ Reanalysis	E1-M3A buoy Monitoring by R/V *SeaDataNet*	2013/05–2015/01 2010/03–2015/01 Climatology	3 h 1 m 1 m
Chl *a*	In situ In situ	E1-M3A buoy Monitoring by R/V	2013/05–2014/06 2010/03–2015/05	3 h 1 m
Cloud fraction & optical thickness	Satellite	NASA	2015/02–2015/03	1 d

countered when measuring zooplankton with upward looking ADCPs and should be treated with caution in acoustical studies of zooplankton.

2.5 Hydrology of the Cretan Sea

The ADCP site is located at the center of the semi-permanent dipole of the Cretan Sea, which consists of a cyclone to the east and an anticyclone to the west of the observatory (Korres et al., 2014; Theocharis et al., 1999). Low frequency variability at the study site is controlled by the intensity and the vertical extent of the dipole as reported by Cardin et al. (2003). Four water masses fill the surface and subsurface layers of the Cretan Sea. Modified Atlantic Water (MAW, salinity $(S) = 38.5$–38.9 psu) fills the 20–100 m layer. Cretan Intermediate Water and Levantine Intermediate Water, which have similar characteristics (CIW & LIW, potential temperature $(\theta) = 14.9$–$15.1\,^{\circ}$C, $S \sim 39.0$–39.1 psu) fill the 200–500 m layer. Transitional Mediterranean Water (TMW, $\theta = 14.2\,^{\circ}$C, $S = 38.92$ psu), a mixture of Levantine Intermediate Water and Eastern Mediterranean Deep Water enters through the Cretan straits and its core lies at the 500–800 m layer (Georgopoulos et al., 2000; Velaoras et al., 2013) or deeper (Velaoras et al., 2015). Below the TMW lies the Cretan Deep Water, a water mass argued to have local (Theocharis et al., 1999) or north/central Aegean origin (Gertman et al., 2006; Zervakis et al., 2000). Inflow of Atlantic water (Theocharis et al., 1999), typically during late summer, causes a salinity minimum at the subsurface layer.

3 Results

3.1 Environmental conditions at the study site

Sea surface temperature ranged seasonally from 15 to 26 °C and salinity ranged from 38.8 to 39.5 psu (Fig. 3b and c). The salinity of the deeper layers ranged from 38.9 to 39.1 psu. The lowest temperatures were observed during February and March, while the highest temperatures were seen during August and September. The seasonal cycle of temperature penetrated down to 100 m and the permanent thermocline extended down to 350 m (Fig. 3b). Salinity also exhibited a seasonal cycle down to 100 m, but the seasonal signal dominated the salinity variations of the upper part of the water column (Fig. 3c). The highest salinity values were observed during calm, cloud free summer days. A salinity minimum between the surface and 100 m depth was also observed in Fig. 3c. Deep casts (Fig. 3e and f) revealed a continuous change of the water column towards fresher and colder values between 250 and 1000 m, especially from 2012 to 2016, which points to intensified horizontal motion of the subsurface layers. The temperature at the depth of the deep scattering layer around 450 m (based on the available data set; Fig. 3d, e and f), ranged from 14.55 to 14.9 °C and the salinity from 38.98 to 39.04 psu.

At the study area, prevailing winds blew from north to northwest (Fig. 4a). Short-term variability of air temperature during winter was larger, due to strong northerly winds, which caused the air temperature to drop below 10 °C. Latent heat loss typically ranged between 100 and 200 W m^{-2}. Sensible heat flux also resulted in a net loss, but it was negligible from March to October. During the rest of the year typical values were less than 50 W m^{-2}. Sensible heat loss significantly contributed to the flux budget when wind stress became larger than 0.2 Pa (average wind stress of the com-
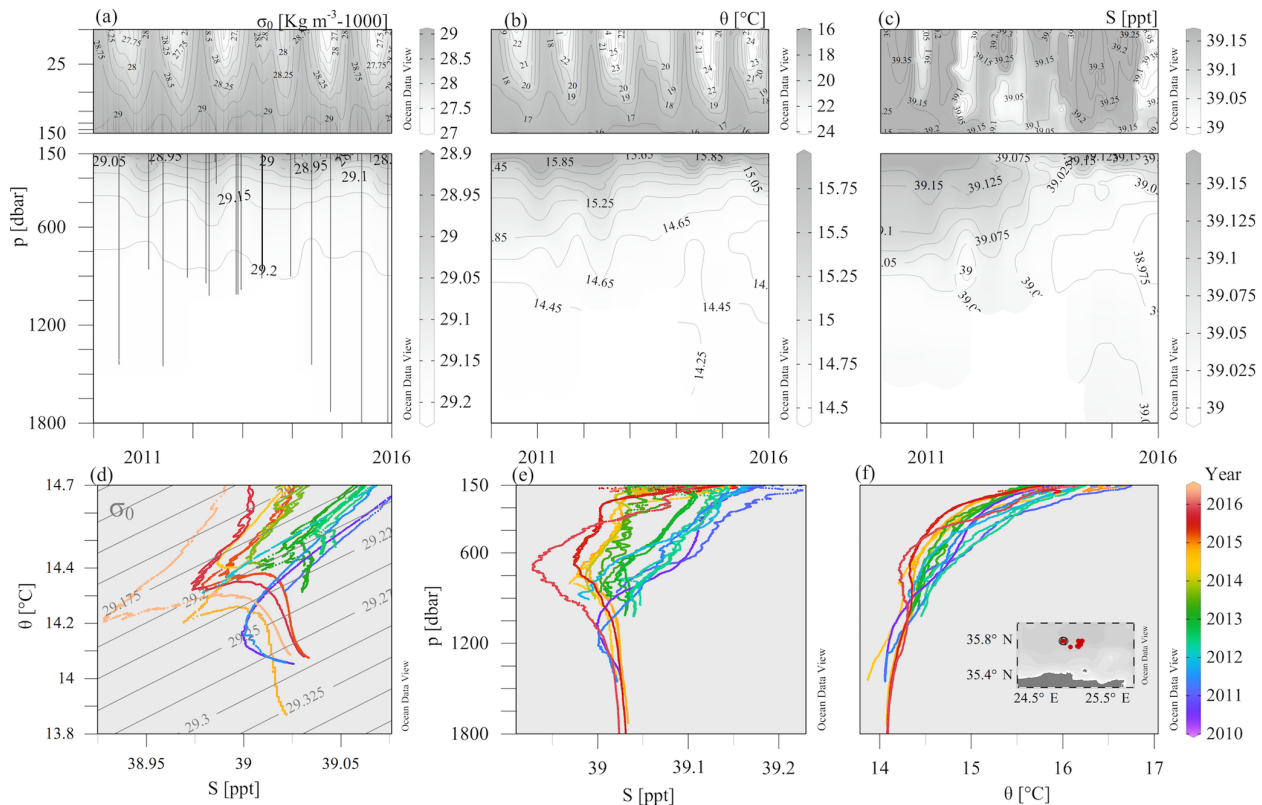
Figure 3. CTD casts collected during monitoring and maintenance visits to the E1-M3A observatory site with HCMR research vessels from 2010 to 2016. Time–depth plots of potential density anomalies (σ_0) **(a)**, potential temperature (θ) **(b)** and practical salinity (S) **(c)**. θ–S plot **(d)** and vertical profiles of S **(e)** and θ **(f)** are colored according to the date to reveal temporal trends.

plete data set was 0.082 Pa). Wind stress during December 2013 was more than 0.2 Pa on average, while peak values of 0.8 Pa were also observed. Consequently, the monthly average sensible heat flux was about $100\,\mathrm{W\,m^{-2}}$ and peak values were about $300\,\mathrm{W\,m^{-2}}$. Latent heat during that period peaked at $600\,\mathrm{W\,m^{-2}}$. Similar atmospheric conditions that favored convection of the upper 100 m of the water column were observed from 10 to 22 February 2015.

Average water velocity from the surface down to 50 m was $0.29\,\mathrm{m\,s^{-1}}$ towards the south-southeast and was invariant with depth. The layer between 50 and 350 m depth was characterized by a diminishing vertical shear that was largest between a depth of 50 and 150 m and vanished below 400 m (Fig. 4d, where only the fourth deployment is displayed, since the larger bin size had caused an underestimation of the high vertical wavenumber shear in previous deployments). The average current speed below 350 m was $0.06\,\mathrm{m\,s^{-1}}$. The direction of the axis of maximum variance between the surface and 50 m was south-southeast and gradually turned to south-southwest at 200 m depth. Currents were also less unidirectional with depth. The strong currents of the surface layer exhibited the least directional variability (Fig. 4b and c). High frequency variability at the site consisted of inertial and tidal currents, which accounted for a small portion

of the total variance (less than 8 %) even though the inertial motions were dominant over short periods.

During the study period the core of the DCM was observed between 70 and 120 m and its vertical extent was around 60 m (Fig. 5a). On average, the largest chlorophyll values were observed at the buoy's 75 and 100 m sensors (Fig. 5b). Furthermore, at these depths, the short-term variability was comparable to the variability due to the annual cycle, while for the 20 and 50 m sensors the seasonal variability was dominant. The DCM formed from February to April and was usually destroyed by October (see changes of the depth range for which the chlorophyll concentration is above 70 % of the maximum value in Fig. 5a).

3.2 Scattering and migrating groups of organisms

The results of the four ADCP deployments over a total duration of 2.5 years (Fig. 6) provided a wealth of information about the scattering organisms and their movement in the water column. Characteristics that are easily visible in Fig. 6 include the presence of a deep layer of scatterers (unfortunately this was only visible in the last deployment, as only then was the ADCP placed deep enough to record it) and a seasonal and a monthly (moon) cycle.
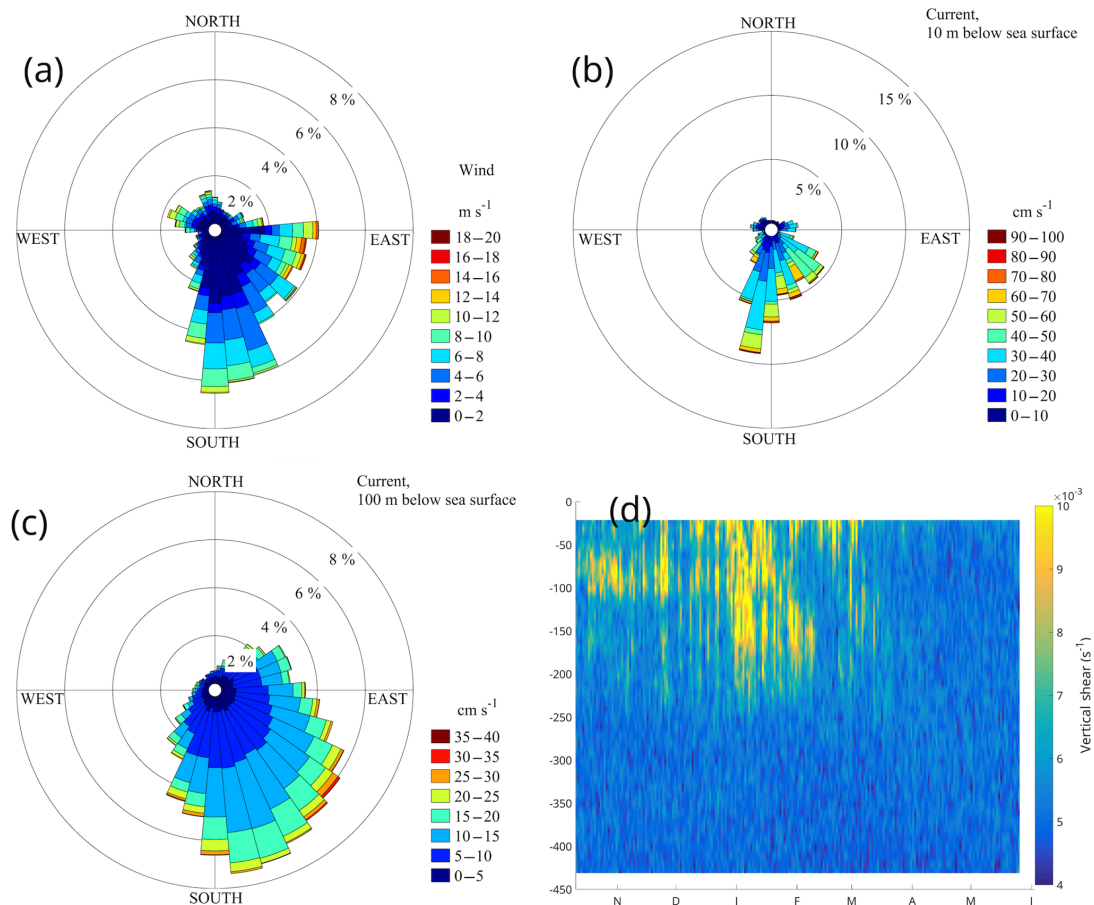
Figure 4. Rose diagrams of wind **(a)** and surface (10 m depth) currents from the buoy's ADCP (400 kHz downward looking) **(b)**, subsurface currents at 100 m depth from the upward looking 75 kHz ADCP **(c)** and vertical shear from the fourth deployment **(d)**. The direction in panels **(a)**, **(b)** and **(c)** point to the direction of the flow.

A closer examination of daily backscatter patterns (Fig. 7) allowed for the categorization of the scattering organisms into four groups according to their migration patterns; this was undertaken on the basis of distinguishable trails of volume backscatter measurements from the ADCP. Three of the groups exhibited a daily migrating pattern, while the fourth remained at a constant depth. The first group (group A hereafter) did not migrate. It was found at 400–450 m, and it formed a deep scattering layer (Fig. 7c).

Group B (Fig. 7) followed the normal DVM pattern, i.e., it moved close to the surface at dusk and returned to the parking depth at dawn, where it stayed during the day. This group spent the daytime at a depth of 400–450 m and the nighttime between 150 m and the surface (Fig. 7). When at the bottom of the seasonally varying daytime parking layer (60–160 m), its vertical velocity decreased; however, it was still moving towards the surface. The bottom of the daytime parking layer was identified by the deceleration of upward movement and the subsequent increase of S_v (Fig. 7), as the zooplankton spent more time in a particular cell when moving at a lower speed. The change in the depth of the bottom of the daytime parking layer of group B was in good agreement with the time variation of the depth of the maximum chlorophyll concentration.

The backscatter coefficient at any certain depth, as long group B was above that depth, was larger during nighttime than daytime (Fig. 7). The exception to this rule was the deep scattering layer. The result was the "curtain" shape of S_v seen in Fig. 7, which implies that a part of the zooplankton that form group B spread through the entire 50–400 m water column while migrating. The smallest S_v values, close to the system noise floor, were observed between 250 and 300 m, when group B was found at the parking depth.

Between 300 and 350 m, S_v never fell close to the noise floor (Fig. 7c), even in the absence of group B during daytime. This points to the presence of scatterers, which indicates a third group of organisms (group C hereafter). Group C migrated from 350 to 300 m or from 250 to 200 m depending on the time of year.
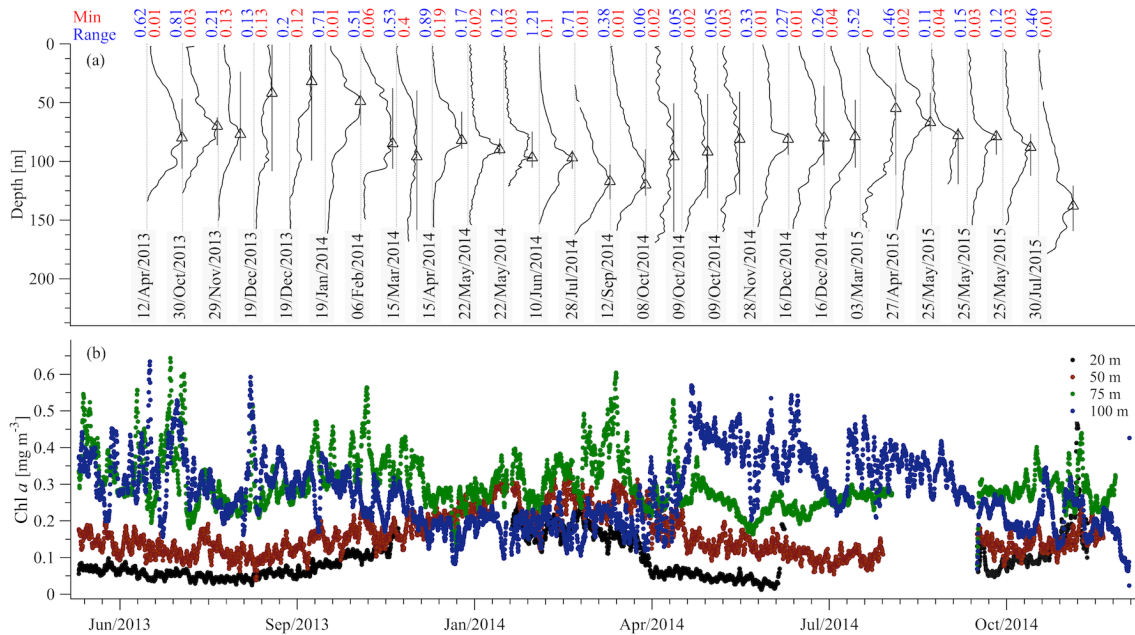
Figure 5. Chlorophyll concentration from the CTD casts **(a)** and the E1-M3A CTD sensors **(b)**. The casts show the vertical distribution of the chlorophyll concentration in the water column (normalized, solid black lines). The minimum value of each cast is denoted by the vertical grey line and the maximum value of each cast is denoted by the black triangle. The black bars around the triangles denote the depth range for which the chlorophyll concentration is above 70 % of the maximum value of the cast. The minimum value and the range of the original chlorophyll values (in mg m^{-3}) are shown above each cast in red and blue, respectively. The E1-M3A chlorophyll data are low passed with a one-day running mean filter.

At shallower depths a fourth group was observed (Fig. 7, Group D), which spent most of the daytime at a depth between 180 and 240 m and during the night it moved to more shallow depths of between 60 and 90 m, where its trails met with those of group B. This was close to the depth where the layer with the largest concentration of phytoplankton throughout most of the year was observed. The backscatter signal of group D was not as strong as that of group B; however, its trail was generally easily distinguishable during its period of upward motion, as a secondary thin strong S_v trail, shallower than the one caused by group B; this was less obvious during the downward motion (Fig. 7). This signal was present in all deployments, but not throughout each deployment, and its characteristics, such as depth and slope, were consistent between deployments.

3.3 Migration timing, duration and velocity

The duration of strong migration did not change with time, with two hours spent each way (four hours in total) (Fig. 8a). Descent was symmetrical with respect to the sunrise; it started one hour before and ended one hour after sunrise (Fig. 8a). Ascent started half an hour before and ended one and a half hour after sunset (Fig. 8a). Depth-averaged velocities during the strong migration period were about 3 cm s^{-1}. While the duration of the strong migration was constant, the migrating velocity changed seasonally, following the dura-

tion of the day which, at 35° longitude, lasts 9.8 h on winter solstice and 14.5 h on summer solstice. This is clearly shown in Fig. 8b, despite the fact that the velocities are quite noisy. Downward velocity was slightly higher than the upward velocity – by almost 1 cm s^{-1} on average (Fig. 8b).

Monthly variability was observed at the depths at which strong downwards migration started (speeds higher than 2.5 cm s^{-1}) (Fig. 9). Furthermore, in Figs. 9 and 10 it can be seen that zooplankton did not migrate at a constant velocity with depth. The highest upward velocities, close to 6 cm s^{-1} were recorded between 200 and 300 m. The highest downward velocities were recorded between 250 and 350 m (Fig. 10). Since group B traveled the longest distance in the course of a day, the largest vertical velocities recorded, especially between 200 and 350 m, might be due to the migration of group B. At a depth of 200 m the ADCP recorded relatively small vertical velocities, about 2 cm s^{-1} (Figs. 9 and 10, all panels), which distorted the vertical profile that would be expected from group B, unless group B decelerated at the bottom of the photic zone. The dispersion of the vertical velocity around the average value at that depth was much less than all the other depths (Fig. 10, all panels).

It was not possible to distinguish the velocity of group B from the velocity of group C, as their S_v trails overlapped during migration. However, utilizing the S_v trails attributed to groups B and D it was possible to distinguish the velocity
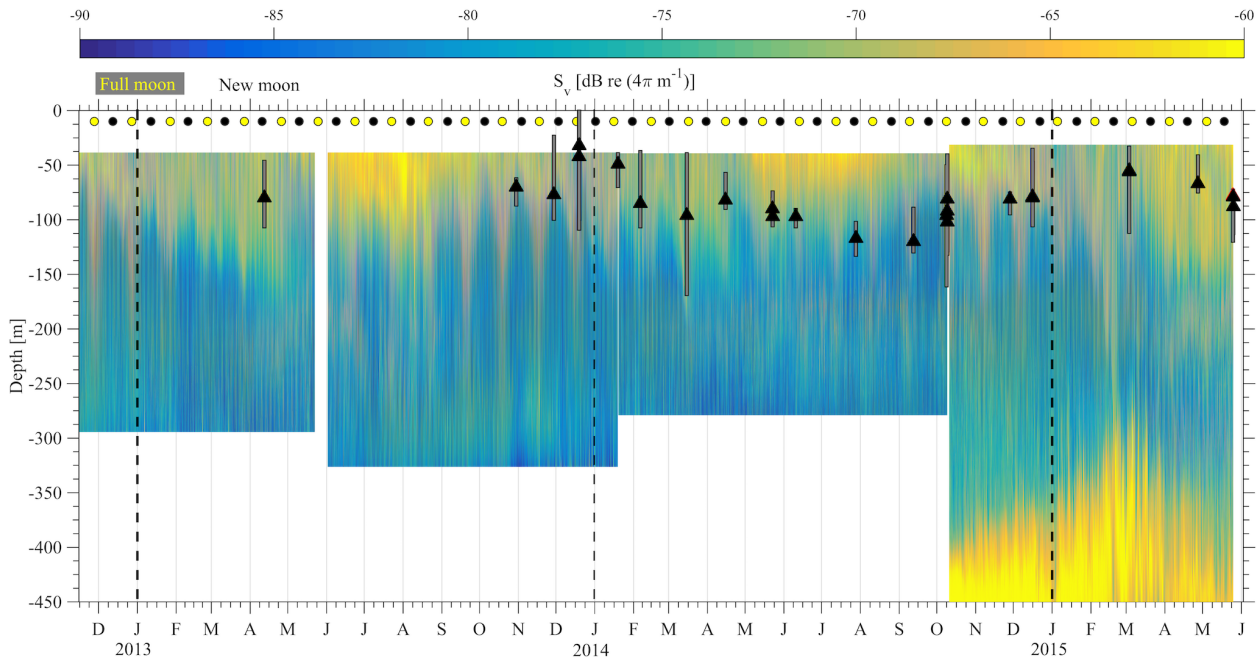
Figure 6. The backscatter coefficient for all ADCP deployments is shown. The beginning of a year is denoted by a dashed vertical line. The yellow and black circles denote the dates of the full and new moons, respectively. The maximum chlorophyll value of available casts is denoted by the black triangle. The gray bars around the triangles represent the depth range for which the chlorophyll concentration is above 70 % of the maximum value of the cast.
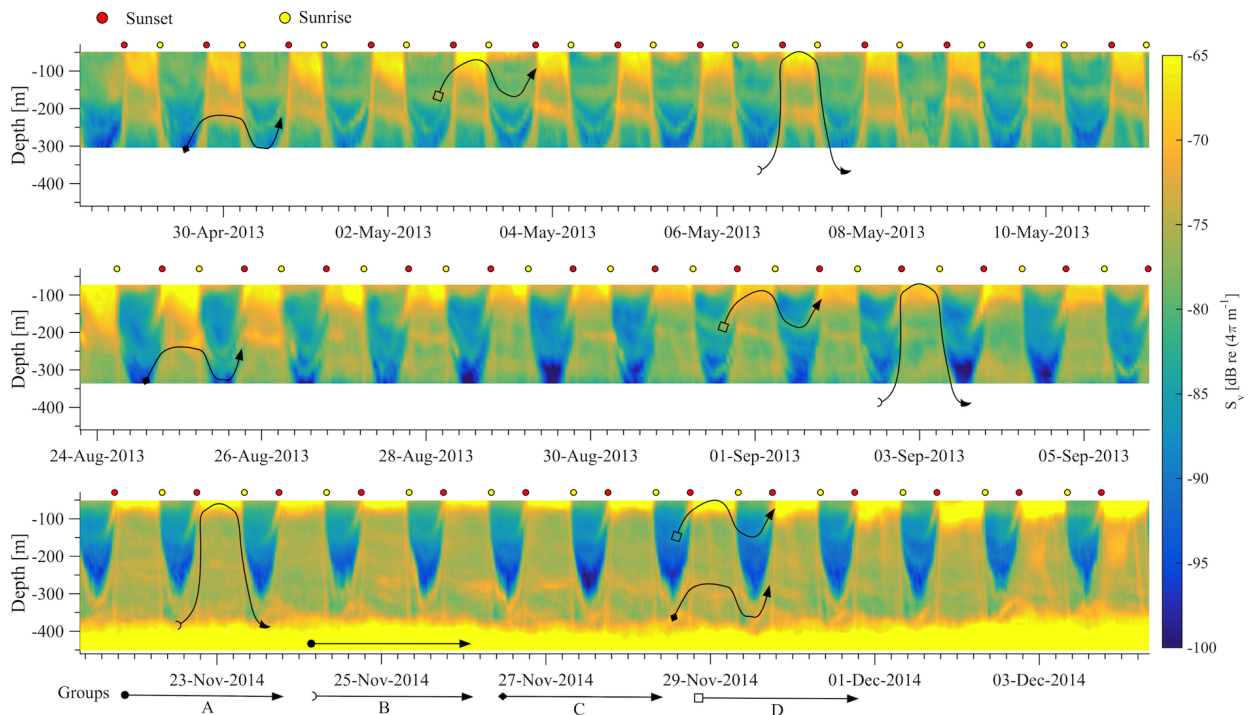

Figure 7. Hand drawn trails of S_v attributed to groups of planktonic and micronektonic organisms.

Figure 8. Instantaneous depth-averaged vertical velocities of daily segments of ADCP measurements between 350 and 50 m **(a)**, following Jiang et al. (2007). Sunrise and sunset times are superimposed. Average of the three highest upward and downward velocity values per day **(b)**. The hours of fast zooplankton motion are also shown.

of group D. The time average vertical velocities and S_v relative to sunrise and sunset hours showed that secondary peaks of S_v attributed to group D were accompanied by a small increase in vertical speed (Fig. 11, all panels). According to the time average velocity measurements in Fig. 10a and b, group D migrated at an average velocity of about $0.2\,\mathrm{cm\,s^{-1}}$. The migrating velocity of group D, calculated indirectly using the trails of S_v (Fig. 11c and d), was about $0.4\,\mathrm{cm\,s^{-1}}$. The depth averaged migrating velocity of $3\,\mathrm{cm\,s^{-1}}$, recorded by the ADCP and attributed to group B, was consistent with the indirect calculation of the migrating speed of group B based on the distance traveled and the duration of its migration (about $3.5\,\mathrm{cm\,s^{-1}}$).

3.4 Effect of an extreme meteorological event

Three successive harsh weather events were observed from 10 to 13, from 17 to 21 and from 23 to 25 February 2015. The sky was mostly overcast (Fig. 12a), the air temperature dropped to $7.5\,^{\circ}\mathrm{C}$ (Fig. 12b), the wind speed reached $15\,\mathrm{m\,s^{-1}}$ and wind gusts exceeded $20\,\mathrm{m\,s^{-1}}$ (Fig. 12c). The third event was shorter than the first two and caused an increase in the air temperature. The homogenization of the water column prior to the first event did not exceed a depth of 50 m (as shown from the E1-M3A time series); however, the nearest (in time) available CTD cast on 3 March revealed that the first 100 m of the water column was homogenized.

The zooplankton were distributed from the surface down to 350 m all day long (Fig. 12e), especially during the first two events, although S_v remained larger during nighttime than at daytime above 300 m. Moreover, only small migrating velocities were measured, especially during the first two events (Fig. 12d). During the second event, the core of the deep scattering layer became shallower, moving to a depth of 350 m. After the third event, the pattern of the backscatter coefficient above 300 m returned to "normal" conditions, but the deep scattering layer remained generally shallower and moved coherently in the vertical direction from 450 to 350 m until the 2 April (Fig. 12e). Thus, changes in the deep scattering layer were observed, which were found well below the maximum depth at which the overturning took place.

4 Discussion

4.1 Factors affecting zooplankton migration

DVM of zooplankton has been related to several exogenous and/or endogenous factors (review by Ringelberg, 2010). In the present study, light intensity seemed to be the major factor affecting the zooplankton migration on daily, monthly and annual timescales. Light can act as an endogenous (entraining circadian rhythms) or exogenous factor controlling DVM. Several hypotheses attempt to explain the exogenous
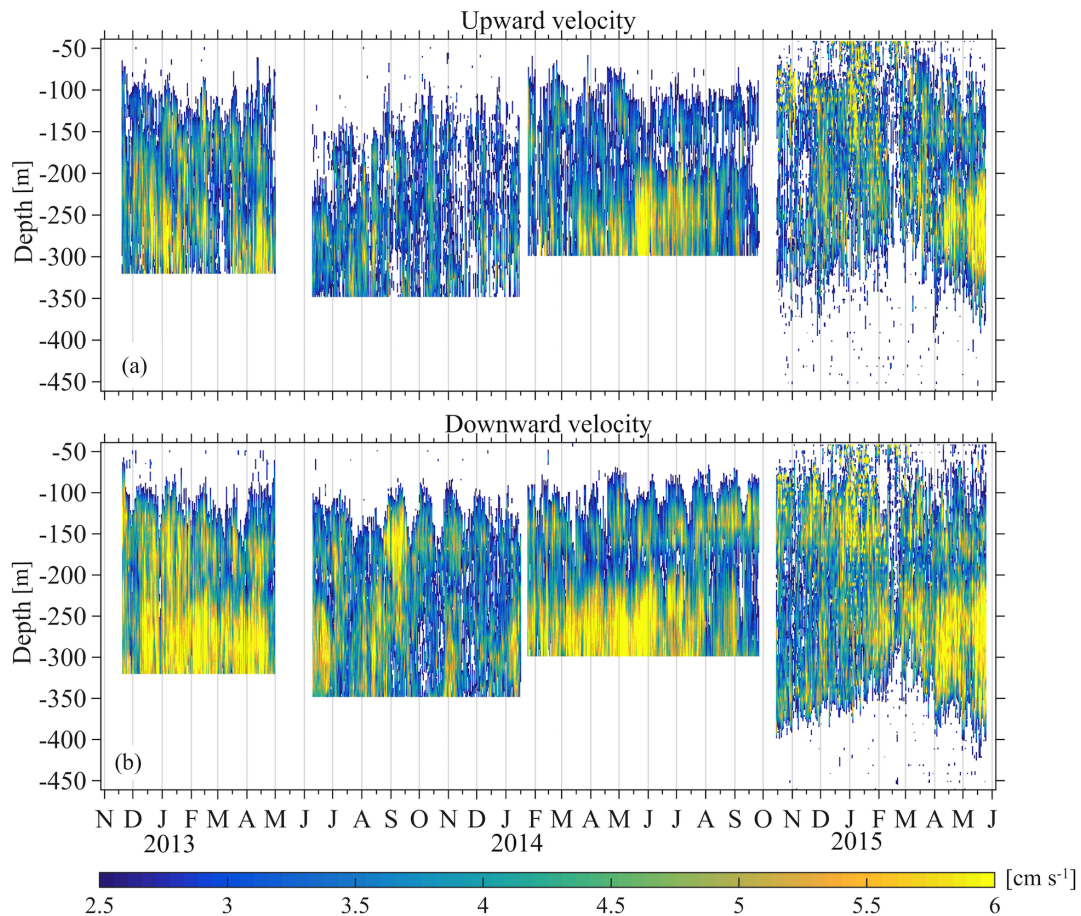
Figure 9. Large upward **(a)** and downward **(b)** velocity, attributed to the migration of zooplankton.

role of light. According to the rate of change hypothesis, the variation in the relative rate and direction of changes in light intensity is the cue to initiate DVM, whereas light also acts to orient and control DVM (Cohen and Forward, 2009).

A scenario that has been proposed to explain DVM is that of a photobehavior formed in order to avoid the damaging effect of solar ultraviolet (UV) radiation. The UV photoreceptors found on zooplankton have supported this (Williamson et al., 2011). However, this mechanism fails to explain the maximum depth of DVM in our case, as UV radiation in the eastern Mediterranean reaches its maximum value at a depth of 50 m (Tedetti and Sempéré, 2006).

Another approach to explain DVM proposes a photobehavior attempting to balance the need of feeding, with avoiding visual predators. Therefore, DVM as a photobehavior should consider the rate of change of light combined with the rate of change of food abundance and kairomones (released by predators and detected by zooplankton). In order to maximize the detection of downwelling light, DVM organisms have adapted their maximum visual sensitivities to wavelengths of about 450–470 nm (although species with photosensitivity to wavelengths larger than 470 nm have been re-

ported as an additional adaptation to bioluminescent emissions) (review by Cohen and Forward, 2009).

According to the results presented here, during full moon the zooplankton prey almost 50 m deeper than during the new moon, which could be a possible behavioral response to increased light conditions. Twilight effects on DVM using data from a downward looking 300 kHz ADCP measuring from the surface down to 80 m were also reported by Bozzano et al. (2014) in the Ligurian Sea.

Furthermore, changes in migration depth and speed have been correlated to cloudiness. Amplitude changes of the extent of DVM due to changes in cloudiness can also be found in the results of Pinot and Jansá (2001). Cloudiness may have an indirect effect on migrants, as the phytoplankton production and the related available prey concentration become lower under lower light conditions. In addition, the prey is spread downward due to convection. Thus, the migrants have to spread in a larger water column in order to obtain a sufficient amount of prey.

Another factor that seemed to affect migration was Chl *a* concentration and location. The seasonally varying zooplankton daytime parking layer extended from the surface
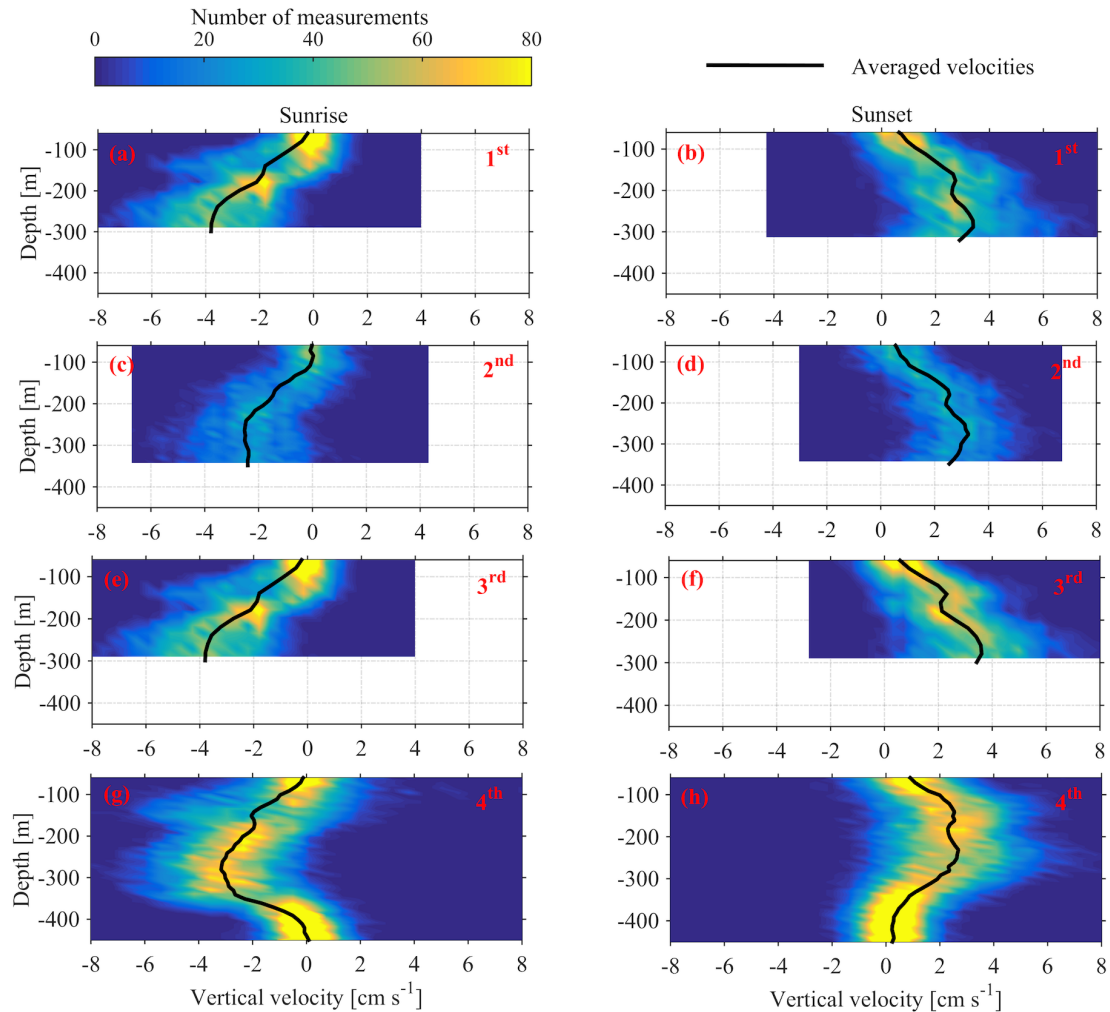
Figure 10. Depth distributions of the vertical velocities, measured 1 h before and 1 h after sunset and sunrise. The time average velocity at each depth is superimposed. Each row of panels refers to one deployment (first, second, third and fourth). The first column of panels corresponds to sunrise and the second column to sunset.

down to a maximum depth of 160 m. The bottom of the daytime parking layer was found at an average depth of 100 m. It was recorded deeper from May to July and shallower from November to January. The upward motion of the migrating groups decelerated at the depth of the largest chlorophyll concentration. The largest vertical velocities were recorded during spring, when the seasonal pycnocline started to form. This was the period of the year that the phytoplankton (Chl a) were spread quite homogeneously throughout the upper 160 m of the water column and the DCM was not yet formed.

The fact that the parking depth of the migrating zooplankton groups B and C (which is also the parking depth of the non-migrating group) is found so deep (450 m), cannot be explained by light, phytoplankton prey concentration (since these are zero below 200 m), or a temperature, salinity or density gradient at that depth. Considering that at the parking depth of these groups the vertical shear practically vanishes, and the horizontal currents are the weakest recorded, might indicate an active behavioral adaptation to minimize energy loss by maintaining their position at a depth with minimum turbulence.

4.2 Zooplankton sampling considerations

Local literature does not allow us to clearly identify the taxonomic composition of the migrating assemblages found in the present study. The few published studies that have sampled zooplankton in the epipelagic and mesopelagic layers of the Cretan Sea, were all done with vertical hauls ($\approx 1\,\mathrm{m\,s}^{-1}$) of 200 µm mesh size nets (Mazzocchi et al., 1997; Siokou-Frangou et al., 1997; Siokou et al., 2013). Thus, they are inappropriate to capture organisms that are roughly 5 mm in size, which are the smaller organisms expected to significantly contribute to the backscatter of a 75 kHz ADCP. How-
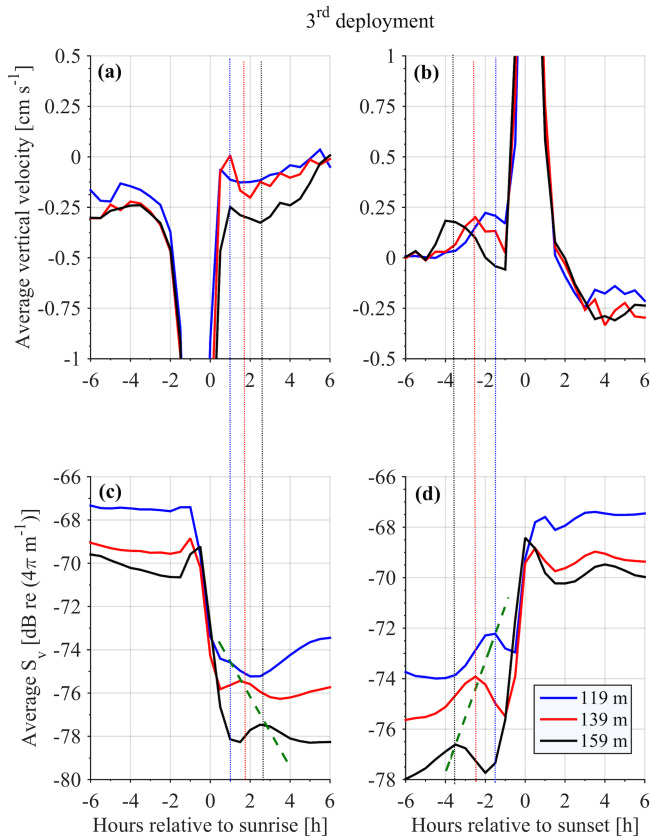
Figure 11. Time average vertical velocity **(a, b)** and S_v **(c, d)** at selected depths during the third deployment. The green dashed line connects the S_v peaks attributed to group D. The vertical dotted lines are used to emphasize the common peaks of vertical velocity and S_v attributed to group D.

ever, it is clear that the assemblages examined in our study include organisms other than copepods, since the biggest copepod species reported in the area (Mazzocchi et al., 1997; Siokou-Frangou et al., 1997; Siokou et al., 2013) reach a maximum size of ≈ 3.5 mm (Razouls et al., 2018). The only qualitative indication about the nature of these migrators in the Cretan Sea is one tow made above the ADCP in December 2013, which captured large organisms (larger than 5 mm) from which the known migrators were decapod larvae, euphausiid larvae, siphonophores and chaetognaths. Indications can also be given by studies targeted at zooplankton migrators in the western Mediterranean Sea by Andersen and collaborators (Andersen and Nival, 1991; Andersen and Sardou, 1992; Andersen et al., 1992; Sardou et al., 1996). Among the several migrant species reported, the most abundant species that were present all year round (euphausiids, siphonophores and decapods) were concentrated above 150 m at nighttime, whereas during daytime the depth of their maximum abundance was found to be seasonally variable (between 300 and 500 m) (Sardou et al., 1996). These groups appeared to have similar behavior to group B in

the present study. Small euphausiids migrated from 420 to 240 m, whereas non-migrants remained below 300 m (Sardou et al., 1996), with similar behavior to groups C and A, respectively, in the present study.

The above work reveals a significant problem associated with the in situ sampling of the abovementioned zooplanktonic groups. Considering that the clear majority of samplings in the area take place during daytime, above 100 m (when groups A, B, C and D are at the deeper part of their migration) and with an inappropriate net type and tow to capture large organisms (as explained above), it is rational to assume that they are misrepresented in the samples. An appropriate sampling strategy, with regular day and night sampling (monthly frequency) and an appropriate net type and tows to study diel and seasonal variation of large organisms, has been carried out in few locations such as the Ligurian Sea (Sardou et al., 1996), the ALOHA site (Al-Mutairi and Landry, 2001) and the BATS site (Jiang et al., 2007; Madin et al., 2001), with significant logistical effort.

4.3 Implications for biogeochemical cycles

If large stocks of large zooplankton actively migrate over significant vertical distances, in an oligotrophic deep system such as the Cretan Sea, new carbon pathways will have to be included in our models, reconsidering the energy flow and the dynamics of the system. In fact, since the carbon inflow (feeding) to the migrant groups comes from lower trophic levels (i.e., phytoplankton) in the euphotic zone, the zooplankton migrators may cause an important active downward vertical flux of matter; thus, the biological pump's efficiency would be increased (review by Frangoulis et al., 2004). The gaps in knowledge for midwater depths severely limit our ability to quantify the efficiency of the biological pump (Robinson et al., 2010). In the Cretan Sea, the lack of knowledge of the role of zooplankton DVM and the functioning of the whole mesopelagic ecosystem may constitute an important knowledge gap regarding the biological pump's efficiency in the area, which requires exploration. Additionally, the observed patterns are expected to have significant implications for the system dynamics, particularly if one considers the oligotrophic character of the Cretan Sea. The observed DVM is expected to act as a transfer mechanism of organic matter (carbon and nutrients) from the euphotic zone to the deeper parts of the water column, overcoming the physical barrier of the pycnocline. This active flux of matter may occur, as the DVM speeds recorded (larger than $3\,\mathrm{cm\,s^{-1}}$) were higher than reported zooplankton faecal pellet sinking speeds (higher than $1\,\mathrm{cm\,s^{-1}}$ for euphausiids – review by Frangoulis et al., 2004). This mechanism will enhance the oligotrophic nature of the mesopelagic layer, since there are no effective mechanisms of very deep-water mixing; there is also a strong decoupling of the surface layers with the deeper parts of the water column. Thus, the surface layers are deprived of important nutrients, although in the actual nutrient budget one
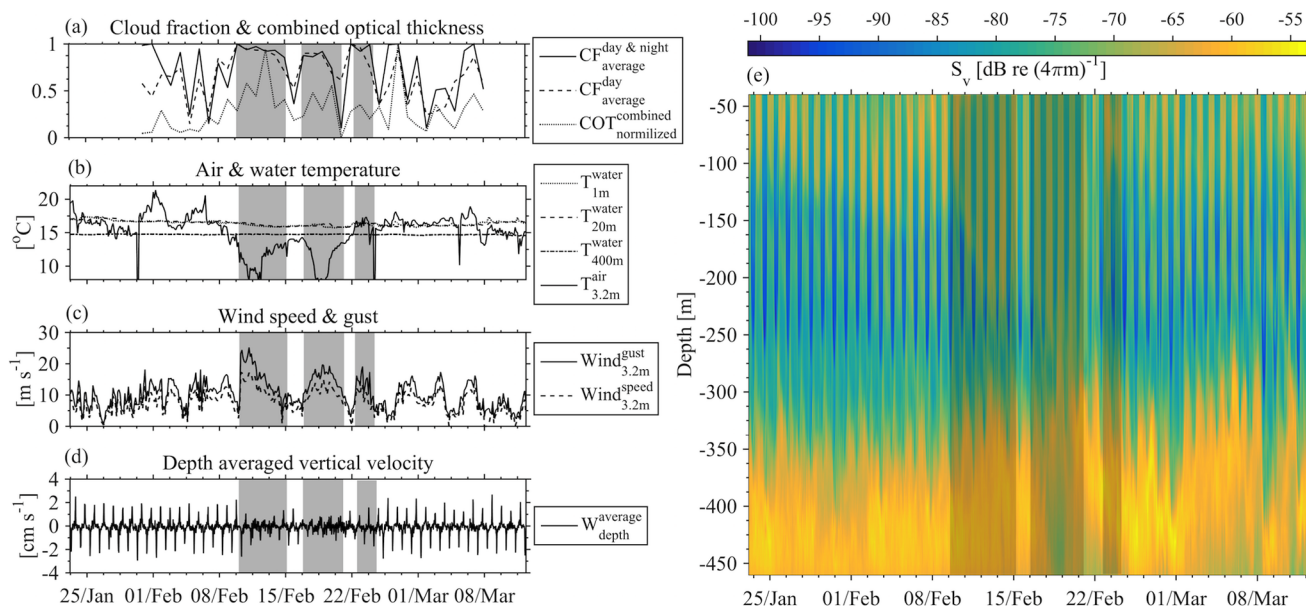
Figure 12. Cloudiness **(a)**, air and water temperature **(b)** and wind conditions **(c)** were examined in comparison to depth-averaged vertical velocities **(d)** and backscatter coefficient **(e)** during February 2015. Grey shaded areas denote the three harsh weather events referred to in the text.

has to take other parameters such as zooplankton excretions at the surface layers etc. into account.

Author contributions. GP, MN and CF designed the experiment and MP, CF, MN, AK and EP carried it out. EP, CF and AK processed the data. EP, CF, AK, GP and VZ prepared the manuscript.

References

Ainslie, M. A. and McColm, J. G.: A simplified formula for viscous and chemical absorption in sea water, J. Acoust. Soc. Am., 103, 1671–1672, https://doi.org/10.1121/1.421258, 1998.

Al-Mutairi, H. and Landry, M. R.: Active export of carbon and nitrogen at Station ALOHA by diel migrant zooplankton, Deep-Sea Res. Pt. II, 48, 2083–2103, https://doi.org/10.1016/S0967-0645(00)00174-0, 2001.

Andersen, V. and Nival, P.: A model of the diel vertical migration of zooplankton based on euphausiids, J. Mar. Res., 49, 153–175, https://doi.org/10.1357/002224091784968594, 1991.

Andersen, V. and Sardou, J.: The diel migrations and vertical distributions of zooplankton and micronekton in the Northwestern Mediterranean Sea. 1. Euphausiids, mysids, decapods and fishes, J. Plankton Res., 14, 1129–1154, https://doi.org/10.1093/plankt/14.8.1129, 1992.

Andersen, V., Sardou, J., and Nival, P.: The diel migrations and vertical distributions of zooplankton and micronekton in the Northwestern Mediterranean Sea. 2. Siphonophores, hydromedusae and pyrosomids, J. Plankton Res., 14, 1155–1169, https://doi.org/10.1093/plankt/14.8.1155, 1992.

Andersen, V., Nival, P., Caparroy, P., and Gubanova, A.: Zooplankton community during the transition from spring bloom to oligotrophy in the open NW Mediterranean and effects of wind events. 1. Abundance and specific composition, J. Plankton Res., 23, 227–242, https://doi.org/10.1093/plankt/23.3.227, 2001.

Ashjian, C. J., Smith, S. L., Flagg, C. N., and Idrisi, N.: Distribution, annual cycle, and vertical migration of acoustically derived biomass in the Arabian Sea during 1994–1995, Deep-Sea Res. Pt. II, 49, 2377–2402, https://doi.org/10.1016/S0967-0645(02)00041-3, 2002.

Bozzano, R., Fanelli, E., Pensieri, S., Picco, P., and Schiano, M. E.: Temporal variations of zooplankton biomass in the Ligurian Sea inferred from long time series of ADCP data, Ocean Sci., 10, 93–105, https://doi.org/10.5194/os-10-93-2014, 2014.

Brierley, A. S., Brandon, M. A., and Watkins, J. L.: An assessment of the utility of an acoustic Doppler current profiler for biomass estimation, Deep-Sea Res. Pt. I, 45, 1555–1573, https://doi.org/10.1016/S0967-0637(98)00012-0, 1998.

Buesseler, K. O. and Boyd, P. W.: Shedding light on processes that control particle export and flux attenuation in the twilight zone of the open ocean, Limnol. Oceanogr., 54, 1210–1232, https://doi.org/10.4319/lo.2009.54.4.1210, 2009.

Cardin, V., Gacic, M., Nittis, K., Kovacevic, V., and Perini, L.: Sub-inertial variability in the Cretan Sea from the M3A buoy, Ann. Geophys., 21, 89–102, https://doi.org/10.5194/angeo-21-89-2003, 2003.

CDO: Climate Data Operators, available at: http://www.mpimet.mpg.de/cdo, last access: 25 July 2018.

CMEMS In Situ Thematic Assembly Centre: IN-SITU_MED_NRT_OBSERVATIONS_013_035, available at: http://marine.copernicus.eu/services-portfolio/access-to-products/?option=com_csw&view=details&product_id=INSITU_MEDNRTOBSERVATIONS_013_035, last access: 25 July 2018.

Cohen, J. H. and Forward, R. B.: Zooplankton diel vertical migration – A review of proximate control, Oceanogr. Mar. Biol., 47, 77–110, https://doi.org/10.1201/9781420094220.ch2, 2009.

Costello, J. H., Pieper, R. E., and Holliday, D. V.: Comparison of acoustic and pump sampling techniques for the analysis of zooplankton distributions, J. Plankton Res., 11, 703–709, https://doi.org/10.1093/plankt/11.4.703, 1989.

Crise, A., Allen, J. I., Baretta, J., Crispi, G., Mosetti, R., and Solidoro, C.: The Mediterranean pelagic ecosystem response to physical forcing, Prog. Oceanogr., 44, 219–243, https://doi.org/10.1016/S0079-6611(99)00027-0, 1999.

Deines, K. L.: Backscatter estimation using Broadband acoustic Doppler current profilers, in: Proceedings of the IEEE 6th Working Conference on Current Measurement, San Diego, USA, 11–13 March 1999, 249–253, 1999.

D'Ortenzio, F. and Ribera d'Alcalà, M.: On the trophic regimes of the Mediterranean Sea: a satellite analysis, Biogeosciences, 6, 139–148, https://doi.org/10.5194/bg-6-139-2009, 2009.

Flagg, C. N. and Smith, S. L.: On the use of the acoustic Doppler current profiler to measure zooplankton abundance, Deep-Sea Res., 36, 455–474, https://doi.org/10.1016/0198-0149(89)90047-2, 1989.

Forward R. B.: Diel vertical migration: Zooplankton photobiology and behaviour, Oceanogr. Mar. Biol., 26, 361–393, 1988.

Fragopoulu, N. and Lykakis, J. J.: Vertical distribution and nocturnal migration of zooplankton in relation to the development of the seasonal thermocline in Patraikos Gulf, Mar. Biol., 104, 381–387, https://doi.org/10.1007/BF01314340, 1990.

Frangoulis, C., Christou, E. D., and Hecq, J. H.: Comparison of Marine Copepod Outfluxes: Nature, Rate, Fate and Role in the Carbon and Nitrogen Cycles, Adv. Mar. Biol., 47, 253–309, https://doi.org/10.1016/S0065-2881(04)47004-7, 2004.

Georgopoulos, D., Chronis, G., Zervakis, V., Lykousis, V., Poulos, S., and Iona, A.: Hydrology and circulation in the Southern Cretan Sea during the CINCS experiment (May 1994–September 1995), Prog. Oceanogr., 46, 89–112, https://doi.org/10.1016/S0079-6611(00)00014-8, 2000.

Gertman, I., Pinardi, N., Popov, Y., and Hecht, A.: Aegean Sea Water Masses during the Early Stages of the Eastern Mediterranean Climatic Transient (1988–90), J. Phys. Oceanogr., 36, 1841–1859, https://doi.org/10.1175/JPO2940.1, 2006.

Gordon, R.: Acoustic Doppler Currrent Profiler: Principles of operation, a practical primer, 2nd Edn., Teledyne RD Instruments Inc., San Diego, California, USA, available at: http://misclab.umeoce.maine.edu/boss/classes/SMS_598_2012/RDI_BroadbandPrimer_ADCP.pdf (last access: 25 July 2018), 1996.

Gotsis-Skretas, O., Pagou, K., Moraitou-Apostolopoulou, M., and Ignatiades, L.: Seasonal horizontal and vertical variability in primary production and standing stocks of phytoplankton and zooplankton in the Cretan Sea and the Straits of the Cretan Arc (March 1994–January 1995), Prog. Oceanogr., 44, 625–649, https://doi.org/10.1016/S0079-6611(99)00048-8, 1999.

Hellenic Center for Marine Research – Poseidon Team: PoseidonDataBase, available at: http://poseidon.hcmr.gr, last access: 25 July 2018.

Henson, S. A., Beaulieu, C., and Lampitt, R.: Observing climate change trends in ocean biogeochemistry: when and where, Glob. Chang. Biol., 22, 1561–1571, https://doi.org/10.1111/gcb.13152, 2016.

Heywood, K. J.: Diel vertical migration of zooplankton in the Northeast Atlantic, J. Plankton Res., 18, 163–184, https://doi.org/10.1093/plankt/18.2.163, 1996.

Holliday, D. V.: Extracting bio-physical information from the acoustic signatures of marine organisms, in: Oceanic Sound Scattering Prediction, vol. 5, Plenum Press, New York, USA, 619–624, 1977.

Holliday, D. V. and Pieper, R. E.: Volume scattering strengths and zooplankton distributions at acoustic frequencies between 0.5 and 3 MHz, J. Acoust. Soc. Am., 67, 135–146, https://doi.org/10.1121/1.384472, 1980.

Holliday, D. V., Pieper, R. E., and Kleppel, G. S.: Determination of zooplankton size and distribution with multifre-

quency acoustic technology, ICES J. Mar. Sci., 46, 52–61, https://doi.org/10.1093/icesjms/46.1.52, 1989.

Isla, A., Scharek, R., and Latasa, M.: Zooplankton diel vertical migration and contribution to deep active carbon flux in the NW Mediterranean, J. Marine Syst., 143, 86–97, https://doi.org/10.1016/j.jmarsys.2014.10.017, 2015.

Jiang, S., Dickey, T. D., Steinberg, D. K., and Madin, L. P.: Temporal variability of zooplankton biomass from ADCP backscatter time series data at the Bermuda Testbed Mooring site, Deep-Sea Res. Pt. I, 54, 608–636, https://doi.org/10.1016/j.dsr.2006.12.011, 2007.

Kassis, D., Korres, G., Petihakis, G., and Perivoliotis, L.: Hydrodynamic variability of the Cretan Sea derived from Argo float profiles and multi-parametric buoy measurements during 2010–2012, Ocean Dynam., 65, 1585–1601, https://doi.org/10.1007/s10236-015-0892-0, 2015.

Koppelmann, R., Weikert, H., Halsband-Lenk, C., and Jennerjahn, T.: Mesozooplankton community respiration and its relation to particle flux in the oligotrophic eastern Mediterranean, Global Biogeochem. Cy., 18, 1–10, https://doi.org/10.1029/2003GB002121, 2004.

Korres, G., Ntoumas, M., Potiris, M., and Petihakis, G.: Assimilating Ferry Box data into the Aegean Sea model, J. Marine Syst., 140, 59–72, https://doi.org/10.1016/j.jmarsys.2014.03.013, 2014.

Koulouri, P., Dounas, C., Radin, F., and Eleftheriou, A.: Near-bottom zooplankton in the continental shelf and upper slope of Heraklion Bay (Crete, Greece, Eastern Mediterranean): observations on vertical distribution patterns, J. Plankton Res., 31, 753–762, https://doi.org/10.1093/plankt/fbp023, 2009.

Lavigne, H., D'Ortenzio, F., Ribera D'Alcalà, M., Claustre, H., Sauzède, R., and Gacic, M.: On the vertical distribution of the chlorophyll *a* concentration in the Mediterranean Sea: a basin-scale and seasonal approach, Biogeosciences, 12, 5021–5039, https://doi.org/10.5194/bg-12-5021-2015, 2015.

Madin, L. P., Horgan, E. F., and Steinberg, D. K.: Zooplankton at the Bermuda Atlantic Time-series Study (BATS) station: diel, seasonal and interannual variation in biomass, 1994–1998, Deep Sea Res. Pt II, 48, 2063–2082, https://doi.org/10.1016/S0967-0645(00)00171-5, 2001.

Malanotte-Rizzoli, P., Artale, V., Borzelli-Eusebi, G. L., Brenner, S., Crise, A., Gacic, M., Kress, N., Marullo, S., Ribera d'Alcalà, M., Sofianos, S., Tanhua, T., Theocharis, A., Alvarez, M., Ashkenazy, Y., Bergamasco, A., Cardin, V., Carniel, S., Civitarese, G., D'Ortenzio, F., Font, J., Garcia-Ladona, E., Garcia-Lafuente, J. M., Gogou, A., Gregoire, M., Hainbucher, D., Kontoyannis, H., Kovacevic, V., Kraskapoulou, E., Kroskos, G., Incarbona, A., Mazzocchi, M. G., Orlic, M., Ozsoy, E., Pascual, A., Poulain, P.-M., Roether, W., Rubino, A., Schroeder, K., Siokou-Frangou, J., Souvermezoglou, E., Sprovieri, M., Tintoré, J., and Triantafyllou, G.: Physical forcing and physical/biochemical variability of the Mediterranean Sea: a review of unresolved issues and directions for future research, Ocean Sci., 10, 281–322, https://doi.org/10.5194/os-10-281-2014, 2014.

Mann, K. H. and Lazier, J. R. N.: Dynamics of Marine Ecosystems, Blackwell Scientific Publications Inc., USA, 2006.

Mazzocchi, G. M., Christou, E. D., Fragopoulu, N., and Siokou-Frangou, I.: Mesozooplankton distribution from Sicily to Cyprus

(eastern Mediterranean): 1. General aspects, Oceanol. Acta, 20, 521–535, 1997.

Moriarty, R. and O'Brien, T. D.: Distribution of mesozooplankton biomass in the global ocean, Earth Syst. Sci. Data, 5, 45–55, https://doi.org/10.5194/essd-5-45-2013, 2013.

Nowaczyk, A., Carlotti, F., Thibault-Botha, D., and Pagano, M.: Distribution of epipelagic metazooplankton across the Mediterranean Sea during the summer BOUM cruise, Biogeosciences, 8, 2159–2177, https://doi.org/10.5194/bg-8-2159-2011, 2011.

Petihakis, G., Triantafyllou, G., Allen, I. J., Hoteit, I., and Dounas, C.: Modelling the spatial and temporal variability of the Cretan Sea ecosystem, J. Marine Syst., 36, 173–196, https://doi.org/10.1016/S0924-7963(02)00186-0, 2002.

Petihakis, G., Ntoumas, M., Pettas, M., Frangoulis, C., Kalampokis, A., and Potiris, E.: ADCP data from Poseidon E1-M3A observatory, Zenodo, https://doi.org/10.5281/zenodo.1311695, 2018.

Pinot, J. M. and Jansá, J.: Time variability of acoustic backscatter from zooplankton in the Ibiza Channel (western Mediterranean), Deep-Sea Res. Pt. I, 48, 1651–1670, https://doi.org/10.1016/S0967-0637(00)00095-9, 2001.

Platnick, S., King, M., and Hubanks, P.: MODIS Atmosphere L3 Daily Product. NASA MODIS Adaptive Processing System, Goddard Space Flight Center, https://doi.org/10.5067/MODIS/MOD08_D3.006, 2015.

Postel, L., da Silva, A. J., Mohrholz, V., and Lass, H.-U.: Zooplankton biomass variability off Angola and Namibia investigated by a lowered ADCP and net sampling, J. Marine Syst., 68, 143–166, https://doi.org/10.1016/j.jmarsys.2006.11.005, 2007.

Razouls, C., de Bovée, F., Kouwenberg, J., and Desreumaux, N.: Diversity and Geographic Distribution of Marine Planktonic Copepods, available at: http://copepodes.obs-banyuls.fr/en/index.php, last access: 25 July 2018.

Ringelberg, J.: Diel vertical migration of zooplankton in lakes and oceans: causal explanations and adaptive significances, Springer Netherlands, Dordrecht, 2010.

Robinson, C., Steinberg, D. K., Anderson, T. R., Arístegui, J., Carlson, C. A., Frost, J. R., Ghiglione, J.-F., Hernández-León, S., Jackson, G. A., Koppelmann, R., Quéguiner, B., Ragueneau, O., Rassoulzadegan, F., Robison, B. H., Tamburini, C., Tanaka, T., Wishner, K. F., and Zhang, J.: Mesopelagic zone ecology and biogeochemistry – a synthesis, Deep-Sea Res. Pt. II, 57, 1504–1518, https://doi.org/10.1016/j.dsr2.2010.02.018, 2010.

Saiz, E., Sabatés, A., and Gili, J.-M.: The Zooplankton, in: The Mediterranean Sea: Its history and present challenges, Springer Netherlands, Dordrecht, Netherlands, 183–211, 2014.

Sardou, J., Etienne, M., and Andersen, V.: Seasonal abundance and vertical distributions of macroplankton and micronekton in the Northwestern Mediterranean Sea, Oceanol. Acta, 19, 645–656, 1996.

Schlitzer, R.: Ocean Data View, available at: https://odv.awi.de (last access: 25 July 2018), 2016.

SeaDataNet: Mediterranean Sea – Temperature and Salinity Climatology V1.1, available at: http://dx.doi.org/10.12770/90ae7a06-8b08-4afe-83dd-ca92bc99f5c0, last access: 25 July 2018.

Siokou, I., Zervoudaki, S., and Christou, E. D.: Mesozooplankton community distribution down to 1000 m along a gradient of oligotrophy in the Eastern Mediterranean Sea (Aegean Sea), J. Plank-

ton Res., 35, 1313–1330, https://doi.org/10.1093/plankt/fbt089, 2013.

Siokou-Frangou, I., Christou, E. D., Fragopoulu, N., and Mazzocchi, M. G.: Mesozooplankton distribution from Sicily to Cyprus (eastern Mediterranean): II. Copepod assemblages, Oceanol. Acta, 20, 537–548, 1997.

Siokou-Frangou, I., Christaki, U., Mazzocchi, M. G., Montresor, M., Ribera d'Alcalá, M., Vaqué, D., and Zingone, A.: Plankton in the open Mediterranean Sea: a review, Biogeosciences, 7, 1543–1586, https://doi.org/10.5194/bg-7-1543-2010, 2010.

Skliris, N.: Past, Present and Future Patterns of the Thermohaline Circulation and Characteristic Water Masses of the Mediterranean Sea, in: The Mediterranean Sea, edited by: Goffredo, S. and Dubinsky, Z., Springer, Dordrecht, https://doi.org/10.1007/978-94-007-6704-1_3, 2014.

Tedetti, M. and Sempéré, R.: Penetration of ultraviolet radiation in the marine environment, A review, Photochem. Photobiol., 82, 389–397, https://doi.org/10.1562/2005-11-09-IR-733, 2006.

Theocharis, A., Balopoulos, E., Kioroglou, S., Kontoyiannis, H., and Iona, A.: A synthesis of the circulation and hydrography of the South Aegean Sea and the Straits of the Cretan Arc (March 1994–January 1995), Prog. Oceanogr., 44, 469–509, https://doi.org/10.1016/S0079-6611(99)00041-5, 1999.

Thomson, R. E. and Emery, W. J.: Data Analysis Methods in Physical Oceanography, 2nd Edn., Elsevier, USA, 2001.

Turner, J. T.: Zooplankton fecal pellets, marine snow, phytodetritus and the ocean's biological pump, Prog. Oceanogr., 130, 205–248, https://doi.org/10.1016/j.pocean.2014.08.005, 2015.

van Haren, H.: Internal wave–zooplankton interactions in the Alboran Sea (W-Mediterranean), J. Plankton Res., 36, 1124–1134, https://doi.org/10.1093/plankt/fbu031, 2014.

Varela, R. A., Cruzado, A., and Tintoré, J.: A simulation analysis of various biological and physical factors influencing the deepchlorophyll maximum structure in oligotrophic areas, J. Marine Syst., 5, 143–157, https://doi.org/10.1016/0924-7963(94)90028-0, 1994.

Velaoras, D., Krokos, G., and Theocharis, A.: An internal mechanism alternatively drives the preconditioning of both the Adriatic and Aegean Seas as dense water formation sites in the Eastern Mediterranean, Rapp. Comm. Int. Mer Medit., 40, p. 178, 2013.

Velaoras, D., Krokos, G., and Theocharis, A.: Recurrent intrusions of transitional waters of Eastern Mediterranean origin in the Cretan Sea as a tracer of Aegean Sea dense water formation events, Prog. Oceanogr., 135, 113–124, https://doi.org/10.1016/j.pocean.2015.04.010, 2015.

Wiebe, P. H. and D'Abramo, L.: Distribution of euphausiid assemblages in the Mediterranean Sea, Mar. Biol., 15, 139–149, https://doi.org/10.1007/BF00353642, 1972.

Williamson, C. E., Fischer J. M., Bollens S. M., Overholt E. P., and Breckenridge J. K.: Toward a more comprehensive theory of zooplankton diel vertical migration: Integrating ultraviolet radiation and water transparency into the biotic paradigm, Limnol. Oceanogr., 56, 1603–1623, https://doi.org/10.4319/lo.2011.56.5.1603, 2011.

Wessel, P., Smith, W. H. F., Scharroo, R., Luis, J., and Wobbe, F.: Generic Mapping Tools: Improved Version Released, Eos, Trans. Am. Geophys. Union, 94, 409–410, https://doi.org/10.1002/2013EO450001, 2013.

Zervakis, V., Georgopoulos, D., and Drakopoulos, P. G.: The role of the North Aegean in triggering the recent Eastern Mediterranean climatic changes, J. Geophys. Res.-Oceans, 105, 26103–26116, https://doi.org/10.1029/2000JC900131, 2000.

Zhou, M. and Dorland, R. D.: Aggregation and vertical migration behavior of *Euphausia superba*, Deep-Sea Res. Pt. II, 51, 2119–2137, https://doi.org/10.1016/j.dsr2.2004.07.009, 2004.